



Universiteit
Leiden
The Netherlands

Starlight beneath the waves : in search of TeV photon emission from Gamma-Ray Bursts with the ANTARES Neutrino Telescope

Laksmana-Astraatmadja, T.

Citation

Laksmana-Astraatmadja, T. (2013, March 26). *Starlight beneath the waves : in search of TeV photon emission from Gamma-Ray Bursts with the ANTARES Neutrino Telescope*. *Casimir PhD Series*. Retrieved from <https://hdl.handle.net/1887/20680>

Version: Not Applicable (or Unknown)

License: [Leiden University Non-exclusive license](#)

Downloaded from: <https://hdl.handle.net/1887/20680>

Note: To cite this publication please use the final published version (if applicable).

Cover Page



Universiteit Leiden



The handle <http://hdl.handle.net/1887/20680> holds various files of this Leiden University dissertation.

Author: Astraatmadja, Tri Laksmana

Title: Starlight beneath the waves : in search of TeV photon emission from Gamma-Ray Bursts with the ANTARES Neutrino Telescope

Issue Date: 2013-03-26

PART III

Data analysis

10 *Prospective GRB sources*

IN THIS Chapter the procedure for selecting prospective GRB sources will be described as well as a description of the target GRB proposed to the ANTARES Collaboration to be observed.

10.1 *Selection Procedure*

A NUMBER of GRB events from the past ~ 6 years has been compiled from various GRB catalogues and ranked in order of their expected signal μ_s . The catalogues used to compile the events and the number of GRBs obtained are:

1. *Swift* GRB Table, http://swift.gsfc.nasa.gov/docs/swift/archive/grb_table.html/, 729 GRBs as of 29 January 2012.
2. *Fermi* GRB Table, http://fermi.gsfc.nasa.gov/ssc/observations/types/grbs/grb_table/, 26 GRBs as of 29 January 2012.
3. GRBweb compilation, <http://grbweb.icecube.wisc.edu/> (Aguilar, 2011), 568 GRBs as of 29 January 2012.
4. GRBox, <http://lyra.berkeley.edu/grbox/grbox.php>, 1 GRB (GRB 080109A) that turns out to be an X-ray transient.

In these catalogues, most of the six physical properties required to construct the photon spectrum and to estimate the expected number of signal μ_s are available. Furthermore, whenever available, the properties in the initial catalogue are superseded with those of the values calculated by Butler et al. (2007); Butler, Bloom & Poznanski (2010) for the *Swift* GRBs and from Zhang et al. (2011) for the *Fermi* GRBs. For these papers, the authors have rigorously analyzed the spectra of the detected GRBs and have calculated the values that best fit their spectral profile. If there is still an unknown value, the standard values shown in Table 10.1 are used. These “most likely” values are obtained from the statistical analysis of GRBs measured by Butler et al. (2007); Butler, Bloom & Poznanski (2010).

Par.	Definition	Value
α	spectral index at low energy	1
β	spectral index at high energy	2
ϵ_{pk}	the energy at which the spectrum peaks	400 keV
$L_{\text{bol}}^{\text{iso}}$	isotropic bolometric luminosity	8.9×10^{52} erg
Δt_*	source-frame burst duration	30 s
z	redshift	0.97

Table 10.1: The standard values of GRB physical properties used to estimate the expected number of signal events μ_s .

The redshifts of each individual GRBs are treated differently depending on the available data. If the redshift is directly measured by a ground-based telescope, this measurement will be immediately used. Unfortunately, due to the transient nature of GRBs, only a small minority of GRBs have measured redshift. If the redshift is unknown, the following scheme is employed in descending order of priority:

1. If the apparent γ -ray flux F_{iso} is measured, I transform this measured flux from the instrument band into the standard bolometric band of 1–10⁴ keV. The transformation is performed by assuming that the bolometric flux is related to the measured flux by

$$F_{\text{iso}}^{\text{bol}} = f_I F_{\text{iso}}^{\text{inst}}, \quad (10.1)$$

where f_I is the conversion factor from the instrument band to the bolometric band. If we know that the photon energy spectrum is in the form of the Band function, then both $F_{\text{iso}}^{\text{bol}}$ and $F_{\text{iso}}^{\text{inst}}$ can be calculated by integrating the Band function $N(\epsilon)$ described in Equation 2.52 in their respective energy band:

$$\int_{1 \text{ keV}}^{10^4 \text{ keV}} d\epsilon N(\epsilon_\gamma) \epsilon = f_I \int_{\epsilon_1}^{\epsilon_2} d\epsilon N(\epsilon) \epsilon, \quad (10.2)$$

where (ϵ_1, ϵ_2) is the energy range of the detector involved. The solution to the integral on both side for $\alpha = 1$ is given in Equation 2.59. However, various values of α have been measured and it is necessary to solve the integral for a general value of α :

$$\lambda_{\text{bol}}(\alpha, \beta, \epsilon_{\text{bk}}, \epsilon_1, \epsilon_2) = \epsilon_{\text{bk}}^2 (\lambda_{\text{low}} + \lambda_{\text{high}}), \quad (10.3)$$

where

$$\lambda_{\text{low}} = \left(\frac{\epsilon_1}{\epsilon_{\text{bk}}} \right)^{2-\alpha} E_{\alpha-1} \left((\beta - \alpha) \frac{\epsilon_1}{\epsilon_{\text{bk}}} \right) - E_{\alpha-1}(\beta - \alpha), \quad (10.4)$$

$$\lambda_{\text{high}} = \exp(\alpha - \beta) \times \begin{cases} \frac{1}{2-\beta} \left[\left(\frac{\epsilon_2}{\epsilon_{\text{bk}}} \right)^{2-\beta} - 1 \right], & \beta \neq 2, \\ \ln \left(\frac{\epsilon_2}{\epsilon_{\text{bk}}} \right), & \beta = 2, \end{cases} \quad (10.5)$$

where $E_n(x)$ in Equation 10.4 is the exponential integral (Abramowitz & Stegun, 1964)

$$E_n(x) = \int_1^{\infty} dt \frac{e^{-xt}}{t^n}, \quad (n = 0, 1, 2, \dots; \Re x > 0). \quad (10.6)$$

Solving both integrals, the conversion factor f_I can then be obtained.

The redshift is then calculated by assuming that the isotropic bolometric luminosity is $L_{\text{bol}}^{\text{iso}} = 8.9 \times 10^{52}$ erg.

2. If no flux is measured, the most probable value of $z = 0.97$ is used and the bolometric luminosity is assumed to be $L_{\text{bol}}^{\text{iso}} = 8.9 \times 10^{52}$ erg.

The same scheme is also employed to calculate $L_{\text{bol}}^{\text{iso}}$. If a measured redshift is available and the flux is also measured, the luminosity is calculated first by transforming the measured flux to the standard bolometric band, and then use it along with the measured redshift to calculate the luminosity. If any of those values are unavailable, the standard value from Table 10.1 is used.

After all of the six values are determined, we can then proceed by calculating the expected number of signal event μ_s :

$$\mu_s = t_{\text{exp}} \int_0^{\infty} d\epsilon_{\mu} \frac{dN_{\mu}}{d\epsilon_{\mu}}(a, b, T_{90}, \epsilon_{\text{pk}}, L_{\text{bol}}^{\text{iso}}, z, \theta) A_{\mu}^{\text{eff}}(\epsilon_{\mu}), \quad (10.7)$$

where t_{exp} is the exposure time of the data taking and is assumed to be equal to the measured T_{90} or 30 seconds if it is not measured; $A_{\mu}^{\text{eff}}(\epsilon_{\mu})$ is the muon effective area as a function of the muon energy ϵ_{μ} and is already presented in Section 7.2.3; $dN_{\mu}/d\epsilon_{\mu}$ is the muon spectrum of the GRB at detector level, given the six physical parameters of the GRB and its zenith distance θ . It can be calculated using the prescription formulated in Chapters 2–3.

The expected number of background event μ_{bg} parallel with the direction of the GRB is calculated by counting all the events from the reconstructed data that are within the circle of the optimum radius centered on the zenith distance θ of the GRB and weight them according to Equation 8.5.

All the GRBs in the catalogue are selected according to these preliminary criteria:

1. The GRB must occur after the first light of ANTARES, which is on 2 March 2006.
2. The GRB must be above the horizon of ANTARES when it is occurring.
3. $\mu_s \geq 10^{-9}$.

Using these three criteria alone, 14 GRBs satisfying all three criteria are found. They are shown in Table 10.2, sorted in descending order of μ_s . In the last column of this Table the Li & Ma (1983) significance is also calculated. In calculating the Li & Ma significance, the on-time is taken to be equal to T_{90} and the off-time is taken to be 1800 seconds (30 minutes) long.

By looking at the number of expected signal μ_s , it is apparent that the collecting area of ANTARES still too small to observe interesting TeV sources. It was proposed that the top two prospective GRBs will be observed, i.e. GRB 090709A and GRB 070220. Even if in the end we do not find any signal-like events, it possible to set up a confidence limit on ANTARES sensitivity to TeV γ -rays.

Before further analysis of ANTARES data can be performed, an optimum quality cut needs to be found. In order to do this, the number of expected signal and background need to be estimated. To achieve the former, a full Monte Carlo simulation from the top of the atmosphere to the detector volume needs to be performed. The latter can be estimated by analysing the data already obtained by ANTARES in the past years. The upper limit of signal event rate μ_s can be determined by calculating the upper limit of the Feldman-Cousins confidence interval, given the estimated number of background μ_b , the number of observed events n_{obs} and the required confidence limit $\alpha = 90\%$.

Table 10.2: The list of prospective GRBs in which the top 2 were proposed to be unblinded.

No.	Name	α [$^{\circ}$]	δ [$^{\circ}$]	Az [$^{\circ}$]	Alt [$^{\circ}$]	F_{iso} [erg cm $^{-2}$]	a	b	E_{pk} [keV]	T_{90} [s]	z	L_{iso} [10^{52} erg]	μ_{sig}	μ_{bg}	S
1	090709A	289.94	60.73	331.62	25.09	1.55×10^{-3}	0.06 ^b	1 ^c	283.24 ^b	344.85 ^b	0.13/	5.50 ^c	3.72×10^{-4}	0.0516	0.30
2	070220	34.80	68.80	4.68	22.05	5.02×10^{-4}	0.29 ^b	1 ^c	350.45 ^b	150.67 ^b	0.22/	5.50 ^c	3.65×10^{-7}	0.0169	0.18
3	060505	331.77	-27.82	176.54	19.39	9.44×10^{-7}	0.29 ^b	1 ^c	400 ^c	4.00 ^f	0.089 ^f	0.0049 ^f	1.64×10^{-7}	0.0003	0.02
4	080325	277.91	36.52	98.27	68.77	1.06×10^{-4}	0.67 ^b	1 ^c	36.63 ^b	183.92 ^b	0.46 ^f	5.50 ^c	1.48×10^{-7}	0.1221	0.48
5	101225A	0.20	44.57	284.15	75.88	1.90×10^{-6}	0.82 ^a	1 ^c	400 ^c	1088.00 ^a	0.4 ^f	0.21 ^d	8.33×10^{-8}	1.0500	1.28
6	080727C	32.64	64.13	32.60	36.23	1.44×10^{-4}	-0.06 ^b	1 ^c	202.10 ^b	99.84 ^b	0.40 ^f	5.50 ^c	6.12×10^{-8}	0.0331	0.25
7	081022	226.58	12.41	225.37	51.76	9.25×10^{-5}	-0.07 ^b	1 ^c	83.70 ^b	149.60 ^b	0.49 ^f	5.50 ^c	4.46×10^{-8}	0.0733	0.38
8	081126	323.53	48.71	303.49	41.18	1.10×10^{-4}	-0.06 ^b	1 ^c	261.38 ^b	59.60 ^b	0.45 ^f	5.50 ^c	3.80×10^{-8}	0.0240	0.22
9	070616	32.10	56.95	332.06	19.64	4.88×10^{-4}	0.33 ^b	1 ^c	99.47 ^b	443.52 ^b	0.22 ^f	5.50 ^c	2.49×10^{-8}	0.0350	0.25
10	110825A	46.00	13.80	128.84	51.08	5.45×10^{-5}	0.23 ^b	1.04 ⁱ	245.74 ^b	6.90 ^j	0.49 ^f	5.50 ^c	1.94×10^{-8}	0.0033	0.08
11	080319A	206.35	44.08	294.34	45.20	9.46×10^{-5}	0.64 ^b	1 ^c	38.10 ^b	45.63 ^b	0.48 ^f	5.50 ^c	7.26×10^{-9}	0.0195	0.20
12	070704	354.71	66.26	21.78	27.06	1.77×10^{-4}	0.59 ^b	1 ^c	91.91 ^b	384.78 ^b	0.36 ^f	5.50 ^c	4.31×10^{-9}	0.0667	0.35
13	060512	195.75	41.21	275.73	68.31	2.32×10^{-7}	-0.55 ^b	1 ^c	34.50 ^b	8.37 ^b	0.4428 ^d	0.02 ^g	2.73×10^{-9}	0.0055	0.10
14	080515	3.17	32.56	100.02	61.87	4.92×10^{-5}	-0.74 ^b	1 ^c	46.27 ^b	22.05 ^b	0.66 ^f	5.50 ^c	2.31×10^{-9}	0.0135	0.16

^a *Swift* GRB table, http://heasarc.gsfc.nasa.gov/docs/swift/archive/grb_table/

^b Butler et al. 2007, 2010

^c Assumed value.

^d Observation.

^e Calculated from measured fluence and assumed L_{iso} .

^f Calculated from Butler et al. 2007, 2010 fluence and assumed L_{bol} .

^g Adopted from the calculations of Butler et al. 2007, 2010.

^h Calculated from the fluence measured by *Swift*-BAT and assumed L_{bol} .

ⁱ GRBweb, <http://grbweb.icecube.wisc.edu>

10.2 GRB 090907A

GRB 090709A was discovered by the Burst Alert Telescope (BAT)¹ onboard *Swift* on 2009 July 9 at $T_0 = 07:38:34$ UT in $(\alpha, \delta)_{J2000} = (19^{\text{h}}19^{\text{m}}43^{\text{s}}, +60^{\circ}43'37.5'')$ (Morris et al., 2009). *Swift* immediately slewed to the GRB and start also observing the GRB with the X-Ray Telescope (XRT)² starting from $T_0 + 67.8$ s. Several follow-up observations were made soon afterward, among others by the automated PAIRITEL Telescope³ (Morgan, Bloom & Klein, 2009) in the infrared, the Palomar Observatory 60-inch (P60) telescope (Cenko et al., 2009), and by the Subaru telescope (Aoki et al., 2009).

The redshift of the GRB was not measured. PAIRITEL near-infrared observations and the P60 in the r' and z' band reveals an extremely red afterglow which suggest a very high redshift ($z \sim 10$) GRB. However, spectroscopic analysis of X-ray from the data taken by XMM-Newton⁴ and *Swift* data suggest a moderate redshift between 3.9 to 5.1 (de Luca et al., 2010).

The γ -ray fluence measured by *Swift* was found to be very bright, with measured bolometric fluences in the 1–10⁴ keV band is $120_{-30}^{+20} \times 10^{-6}$ erg cm⁻² (Butler, Bloom & Poznanski, 2010). This bright flux could also be a possible hint to a small redshift of the GRB. Butler (2009) analyzed the high-energy light curve of the GRB and suggests a low to moderate redshift, $z \lesssim 2$.

The power spectrum of the BAT light curve, shown in Figure 10.1, indicates a quasiperiodic signal with a period of 8 seconds (Markwardt et al., 2009). This is the first time such quasiperiodicity was observed in any GRB, which prompted Markwardt et al. (2009) to suggest that GRB 090709A could be of different origin than the standard scenario for a long GRB. The 8 seconds periodicity is typical for Galactic as well as extragalactic magnetars. This quasiperiodicity is however not observed in the power spectrum of the XRT and XMM light curve (Mirabal & Gotthelf, 2009; de Luca et al., 2010). From the BAT light curve it is found that the burst occurred between $T_0 - 66.665$ s and $T_0 + 509.035$ s, with $T_{90} = 300 \pm 105$ s (Butler, Bloom & Poznanski, 2010).

At the ANTARES site which is located at geographical coordinates $(\phi, \lambda) = (42^{\circ}47'56.1'' \text{ N}, 6^{\circ}9'56.5'' \text{ E})$, the local coordinates of the GRB at T_0 is $(Az, Alt) = (331.62^{\circ}, 25.09^{\circ})$. The GRB is lo-

¹ http://heasarc.gsfc.nasa.gov/docs/swift/about_swift/bat_desc.html

² <http://www.swift.psu.edu/xrt/>

³ Peters Automated Infrared Imaging Telescope, <http://www.pairitel.org/>

⁴ X-ray Multi-Mirror Mission, <http://xmm.esac.esa.int/>

The azimuth angle is measured from the celestial North towards the East.

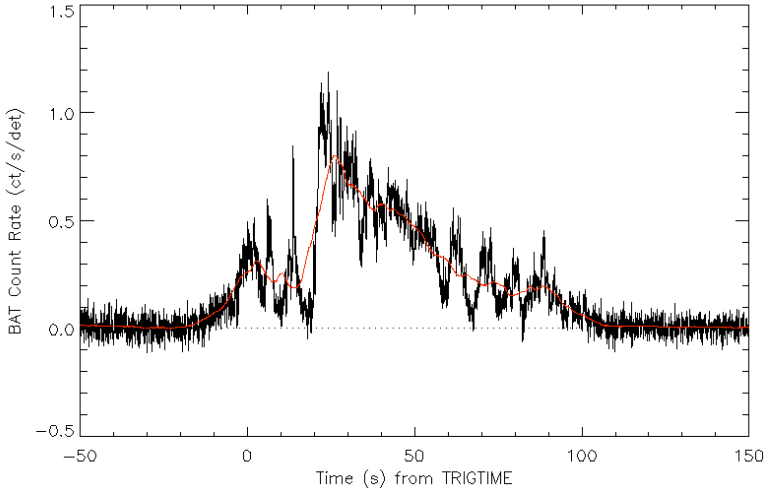


Figure 10.1: The BAT light curve of GRB 090709A, measured in the 15–350 keV band, with a smoothing curve in red performed by Markwardt et al. (2009).

cated rather close to the local horizon, which could result in a reduction of the number of expected muons due to the lengthening of the path traversed through the sea.

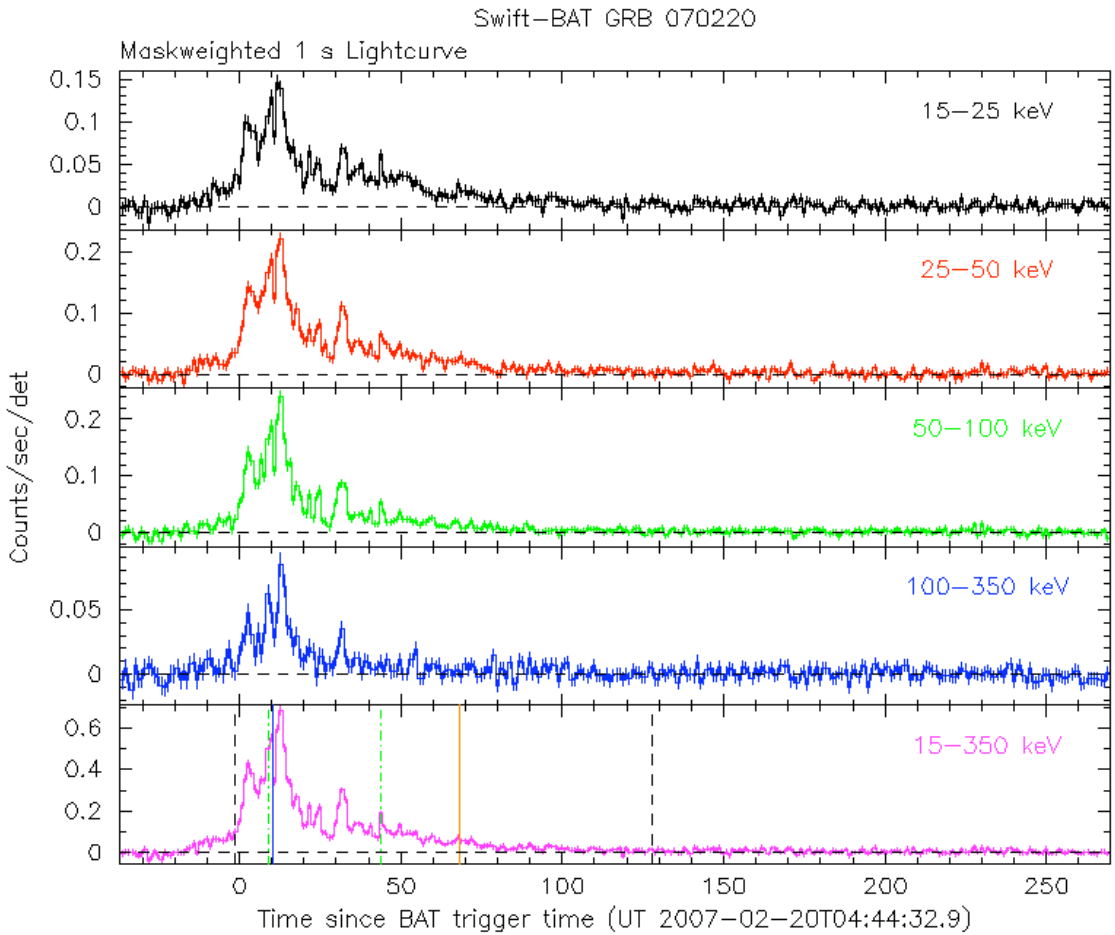
10.3 GRB 070220

THIS GRB triggered BAT on 2007 February 20 at $T_0 = 04:44:33$ UT. *Swift* immediately slewed towards the GRB and observed it with the XRT and the UVOT⁵ starting respectively from $T_0 + 79$ s and $T_0 + 88$ s (Stamatikos et al., 2007a). The 90% confidence level of the GRB’s location is $(\alpha, \delta)_{J2000} = (2^{\text{h}}19^{\text{m}}6.83^{\text{s}}, +68^{\circ}48'16.1'')$, based on XRT observation of the afterglow (Beardmore et al., 2007).

The light curve of GRB 070220 (Figure 10.2) shows a multiple peaked structure with $T_{90} = 129 \pm 6$ s (Parsons et al., 2007). The γ -ray bolometric fluence is measured to be $E_{\text{bol}}^{\text{iso}} = 40_{10}^{30} \times 10^{-6}$ erg cm⁻² (Butler et al., 2007).

Follow-up observations of GRB 070220 were performed in the optical wavelength by the KANATA 1.5 m telescope in Hiroshima (Arai, Uemura & Uehara, 2007) and by the robotic Faulkes North Telescope (Melandri et al., 2007), in the near-infrared by the ART-3 Telescope (Torii, Tanaka & Tsunemi, 2007), and in the radio band

⁵Ultraviolet and Optical Telescope, <http://www.swift.psu.edu/uvot/>



at 8.46 GHz by the Very Large Array (VLA) (Chandra & Frail, 2007). All observations did not find any counterpart to the GRB in the bands observed.

The GRB is also observed by the *Konus* detector (Aptekar et al., 1995) onboard the *Wind* satellite⁶. *Konus* is sensitive to γ -rays in 20 keV–2 MeV, which allows for the high-energy spectral index β to be measured. By fitting the time-integrated energy spectrum of the GRB, $\beta = -2.02^{+0.27}_{-0.44}$ is obtained (Golenetskii et al., 2007). This is very close to the most common value of β . Using this *Konus* spectral parameters, Pelangeon & Atteia (2007) obtained a

Figure 10.2: The BAT light curve of GRB 070220, measured in 4 different energy band and the total energy band in the 15–350 keV energy range (bottom plot). The green and black dotted lines bracket the T_{50} and T_{90} time intervals, respectively, while the blue and orange solid lines bracket the start and end of the slew, respectively. Figure reproduced from Stamatikos et al. (2007b).

⁶ <http://wind.nasa.gov/>

pseudo-redshift of $\hat{z} \sim 2.15 \pm 0.8$. A pseudo-redshift is a redshift indicator proposed by Atteia (2003). The method works by using the observed spectral parameters and the burst duration as an input, and then the redshift is calculated by using the so-called Amati relation (Amati et al., 2002) that found a linear relation between the logarithm of ϵ_{pk} and the logarithm of $E_{\text{iso}}^{\text{bol}}$.

The local coordinates of GRB 070220 at the ANTARES site at T_0 is $(Az, Alt) = (4.68^\circ, 22.05^\circ)$. The GRB is at an altitude close to the local horizon, and given also the predicted redshift of the GRB, most probably there are not many TeV γ -rays that could reach Earth in the first place.

We will simulate the interaction of TeV γ -rays that reach Earth with particles in the atmosphere of the Earth. This will be discussed in the next Chapter.